published in: Phil. Mag. A, 1998, vol. 77, pp. 187-199

KINETICS OF ISOTHERMAL AND NON-ISOTHERMAL PRECIPITATION IN AN Al-6at%Si ALLOY

M.J. Starink and A-M. Zahra

Centre de Thermodynamique et de Microcalorimétrie du CNRS,
13331 Marseille Cedex 3, France

Abstract

A novel theory which describes the progress of a thermally activated reaction under isothermal and linear heating conditions is presented. It incorporates nucleation, growth and impingement, and takes account of temperature dependent solubility. The model generally fits very well to isothermal calorimetry and differential scanning calorimetry data on precipitation in an Al-6at%Si alloy. Analysis of the data shows that two processes occur in this precipitation reaction: growth of large silicon particles and growth of pre-existing small nuclei. Determination of the sizes of Si precipitates by transmission electron microscopy indicates that interfacial energy contributions are small and have a negligible influence on solubility.

1. Introduction

The general aim of the 'theory of transformation kinetics' is the description of amounts transformed during a reaction for all temperature-time (T-t) paths. Often encountered examples of such T-t paths are isothermal holds or heating at a constant rate (linear heating). For the description of an isothermal reaction often the Johnson-Mehl-Avrami-Kolmogorov (JMAK) equation (see e.g. Christian 1975, Cumbrera and Sanchez-Bajo 1995, Sessa, Fanfoni, and Tomellini 1996) is applied. However, there are drawbacks and problems concerning the application of this equation, the main ones being: i) theoretically the validity of the JMAK equation has only been proven for reactions in which the interface moves at a constant velocity (so-called linear growth) (Sessa et al. 1996, Ge Yu and Lai 1996), i.e. it has not been proven for diffusion controlled precipitation reactions, ii) experimental work has shown that many reactions do not conform to JMAK kinetics (Austin and Rickett 1939, Erukhimovitch and Baram 1994, 1995, Starink 1997), and iii) generalisation of the JMAK equation to non-isothermal time paths is not obvious (Cumbrera and Sanchez-Bajo 1995).

Recently, the present authors (Starink and Zahra 1997a) developed a model for the analysis of nucleation and growth type reactions and showed how it can be applied for isothermal (Starink and Zahra 1997c) and linear heating paths (Starink and Zahra 1997a, 1997b). The model incorporates nucleation, growth and impingement, takes account of temperature dependent solubility and distinguishes between diffusion controlled growth and linear growth. This model will be reviewed briefly in Section 3, and in the present work we will critically investigate its validity by comparing its predictions to experiments of precipitation during isothermal and linear heating paths. The

reaction selected for study is the precipitation of Si from the Al-rich matrix in an Al-6at%Si alloy. The main rationale behind this choice is that Al-Si is an ideal model system: it contains only two phases: the Al-rich phase and the Si phase[*], whilst the solubility of Al in the Si phase is negligible (Murray and McAlister 1984). Thus exothermic reactions are always due to the precipitation of Si. Further, high silicon Al-Si alloys with a Si content in excess of ~5at% possess an excellent castability, and as a result this group of alloys is technologically important. The present study will enhance the understanding of heat treatment of these alloys. The linear heating experiments were performed using differential scanning calorimetry (DSC), whilst the isothermal experiments were carried out in a Tian-Calvet isothermal calorimeter. The high sensitivity of the latter ensures that reaction kinetics can be studied with extremely high accuracy. Microstructural investigations were performed using transmission electron microscopy (TEM).

2. Experimental

A conventionally cast, high purity Al-6Si alloy was used (for more details on the alloy, see Starink and Zahra 1997a). Chemical analysis revealed a composition of 5.8 at%Si. For DSC experiments samples were solution treated for 1 h at 550°C and cooled at 200°C/min in a DSC apparatus. For isothermal calorimetry samples were solution treated for 2 h at 550 °C and cooled by introduction into a furnace set at about the temperature for the subsequent calorimetry experiment (furnace cooled).

For DSC experiments disks of 6 mm diameter and 1 mm thickness were used. Scans at heating rates 1.25 to 40 °C/min were performed using a Perkin-Elmer 1020 series DSC7. Details on calibration procedures, baseline correction and correction for heat capacity have been given elsewhere (Starink and Zahra 1997a).

For isothermal calorimetry, batches containing 20 disk shaped samples of 15 mm diameter and 1 mm thickness were prepared and examined in a differential Tian-Calvet microcalorimeter which possesses an excellent base line stability coupled with a high sensitivity (down to a microwatt). The baseline of the apparatus at each temperature was determined by performing experiments with pure Al. Further details of the experimental procedures are presented in Starink and Zahra 1996.

For TEM experiments, specimens were ground to about 100 μm and electropolished in a 3:1 mixture of methanol and nitric acid at -20°C. The foils were examined in a JEOL JEM 2000 microscope operated at 200 kV.

[*] However, some authors (Sakakibara and Kanadani 1990, El Sayed and Kovács 1994, Ozawa and Kimura 1971) have interpreted low temperature resistometric experiments on quenched Al-Si alloys by assuming the existence of precursor phases/states, notably GP zones or Si clusters, but no microstructural evidence of their existence has been reported in literature. Hence, the existence of such precursors is uncertain, and as DSC heat effects due to their formation or dissolution have not been detected in the present work nor in previous work (Starink and Zahra 1997a, Starink 1996), heat effects in our DSC and calorimetry experiments on Al-Si alloys are interpreted as reflecting the precipitation and dissolution of the equilibrium phase only.

3 Nucleation and growth model

It is assumed that, similar to the JMAK model, the transformed volume, V_p, around a single nucleus grows according to:

$$V_p = A\left[G(t - z)\right]^m \qquad (1)$$

where G is the (average) growth rate, A is a constant, z is the time at which the nucleus is formed, whilst m is a constant related to the dimensionality of the growth and the mode of transformation. We will term m the growth exponent. For diffusion controlled precipitation reactions, we will define the transformed volume to be the volume of an imaginary fully depleted area around a precipitate (with the rest of the matrix undepleted) needed to give a precipitate size equal to the real case with a diffusion zone. If all transformed volumes grow without impinging (the so-called extended volume approach), the total transformed volume is given by $V_{ext}(t)$. We introduce the variable $\alpha_{ext} = V_{ext}/V_o$, where V_o is the volume of the sample, and take impingement into account by using (see e.g. Lee and Kim 1990):

$$\frac{d\alpha}{d\alpha_{ext}} = (1-\alpha)^{\lambda_i} \qquad (2)$$

where α is the fraction transformed and λ_i is a (positive) constant. The general solution of Eq. 2 for $\lambda_i \neq 1$ is:

$$\alpha = 1 - \left(\frac{\alpha_{ext}}{\eta_i} + 1\right)^{-\eta_i} \qquad (3)$$

with the impingement exponent $\eta_i = 1/(\lambda_i - 1)$.

Next we introduce the nucleation rate I(z,T). For isothermal paths I will generally be constant or zero. The latter case arises for the limit of I(z) decreasing infinitely fast, and it can, for instance, occur when the number of nucleation sites is limited and all sites are used for nucleation very early on in the transformation (so-called 'site saturation'). For both cases a single general expression can be derived (Starink and Zahra 1997e):

$$\alpha_{ext} = [k(T)\, t]^n \qquad (4)$$

with k(T) a temperature dependent factor determined by A, G and I, or (for the site saturation case) A, G and the density of nuclei. For constant nucleation rate n = m +1, whilst for zero nucleation rate n = m. We will take k(T) as:

$$k(T) = k_o \exp\left[-\frac{E_{iso}}{k_B T}\right] \qquad (5)$$

where E_{iso} denotes the effective activation energy for isothermal experiments, k_o is a constant.

To derive the fraction transformed for a linear heating path it is assumed first that both the growth rate and the nucleation rate can be described by Arrhenius type dependencies. From this follows that α_{ext} can be approximated very accurately as (Woldt 1992, Krüger 1993):

$$\alpha_{ext} \cong \left(\frac{\beta k_B}{E_G} k_c \exp\left[\frac{-E_{eff}}{k_B T} \right] \left(\frac{T}{\beta} \right)^2 \right)^s \tag{6}$$

where

$$E_{eff} = \frac{mE_G + E_N}{m+1} \tag{7}$$

$$s = m + 1 \tag{8}$$

where E_G and E_N are the activation energies for growth and nucleation, respectively, β is the heating rate, k_B is Boltzmann's constant, and k_c is a constant. Also for the case where nuclei are present before the start of the transformation and no further nucleation occurs, Eq. 6 is in good approximation valid. In this case s = m and $E_{eff} = E_G$. This, in combination with Eq. 8, shows that if the assumptions for the derivation of Eqs. 6 to 8 are satisfied and the processes occurring for an isothermal and a linear heating path are the same, s equals n.

If two processes occur whilst impingement of precipitates formed by the two processes is negligible as compared to impingement between precipitates formed by the same process, they essentially occur in independent volumes of the alloy, and one can obtain the sum of two processes simply from a weighted average:

$$\xi = f\,\xi_1 + (1-f)\,\xi_2 \tag{9}$$

where f is the volume fraction of the alloy in which process 1 occurs, whilst ξ is the amount of atoms incorporated in the growing nuclei divided by the maximum amount of atoms that can be incorporated according to the equilibrium phase diagram. (Thus, for isothermal experiments, ξ can be replaced by α in Eq. 9.)

To account for the variation of the equilibrium state with temperature we assume that the variation of the equilibrium or metastable equilibrium concentration, $c_{eq}(T)$, as a result of the increase in temperature is relatively slow as compared to variations in the local concentrations of alloying atoms due to diffusion of atoms. From this follows:

$$\dot{\xi} = \frac{d\xi}{dt} = \frac{d}{dt}\left[\alpha \frac{c_o - c_{eq}(T)}{c_o} \right] A_2 \tag{10}$$

where c_o is the initial concentration of alloying element dissolved (in our alloy solution treated at 550°C c_o = 1.30at%) and A_2 is a constant.

Application of Eq. 10 requires data on $c_{eq}(T)$. For Al-Si this data is readily available (see Ref. 17), and $c_{eq}(T)$ can be described well by a regular solution model (see Van Rooyen and Mittemeijer 1989, Starink 1996), i.e.:

$$c_{Si}(T) = c_{\infty} \exp\left(-\frac{\Delta H_{sol}}{k_B T} \right) \qquad (11)$$

where for Si in Al $c_{\infty} = 33$ and the enthalpy of solution $\Delta H_{sol} = 54$ kJ/mole (= 0.56 eV).

4 Results and discussion

4.1 The Gibbs-Thomson effect investigated by TEM and DSC

An essential element in the model described in the previous section is the solubility of the precipitating phase. The equilibrium solubility of Si in the Al-rich phase is well established and is accurately represented by Eq. 11. However, the size of precipitates can have an important influence on solubility through the Gibbs-Thomson effect, i.e. with decreasing size the interfacial energy will result in an increasing (metastable) solubility. This effect may be all the more important as the Al/Si interfacial energy, $\sigma_{Si/Al}$, is high (about 1.5 J/m^2, see Van Rooyen and Mittemeijer 1989). Hence, before proceeding to the main theme of this paper, a comparison of the presented model with isothermal and linear heating experiments, this possible complication is investigated. To this end, an Al-Si alloy will be studied by TEM and DSC. It was realised that the Al-6Si samples are ill suited for accurate quantitative DSC studies because the high silicon content causes a continuous dissolution effect up to the temperature where the alloy starts melting, which in turn results in a low accuracy in the determination of a baseline. Hence, instead of the Al-6Si alloy, a high purity Al-1.0at%Si alloy (see Starink 1996) was used for the DSC and TEM experiments in this sub-section. It is thought that the sizes of the Si precipitates formed in the two alloys during heat treatment after cooling at -200°C/min will be similar.

The Al-1Si samples were solution treated, cooled at -200°C/min and subsequently heated in the DSC at 5°C/min up to the end of the exothermic effect (at 370°C). The samples were aged for 5 min and for 24 h at 370°C and subsequently quenched. TEM micrographs of the Al-1Si alloy aged for 5 min are presented in Fig. 1. In correspondence with other work on precipitation in Al-Si alloys (Saulnier 1961, Hornbogen, Mukhopadhyay and Starke 1992a, 1992b), this figure shows the presence of precipitates with various shapes. It is well established in the literature that all precipitates are diamond cubic Si-rich phase. By measuring sizes of about 80 equiaxed Si particles over different areas of the sample, the characteristic average diameter was determined to be 117 nm. In the sample aged for 24 h (see Fig. 2) the average diameter of the equiaxed precipitates is 164 nm. Assuming the particles to be approximately spherical, the interfacial energy per mole Si in the precipitate, $E_{Si/Al}$, can be calculated from the relation (see e.g. Van Rooyen and Mittemeijer 1989):

$$E_{Si/Al} = 3\frac{\sigma_{Si/Al}}{\rho_{Si}\, r} \qquad (12)$$

where ρ_{Si} is the atomic density of the Si phase (5×10^{28} atoms/m^3) and r is the radius of the precipitate. If only the equiaxed particles are considered, one finds for the sample aged for 5 min $E_{Si/Al}$ = 0.9 kJ per mole Si, whilst after 24 h $E_{Si/Al}$ = 0.7 kJ per mole Si.

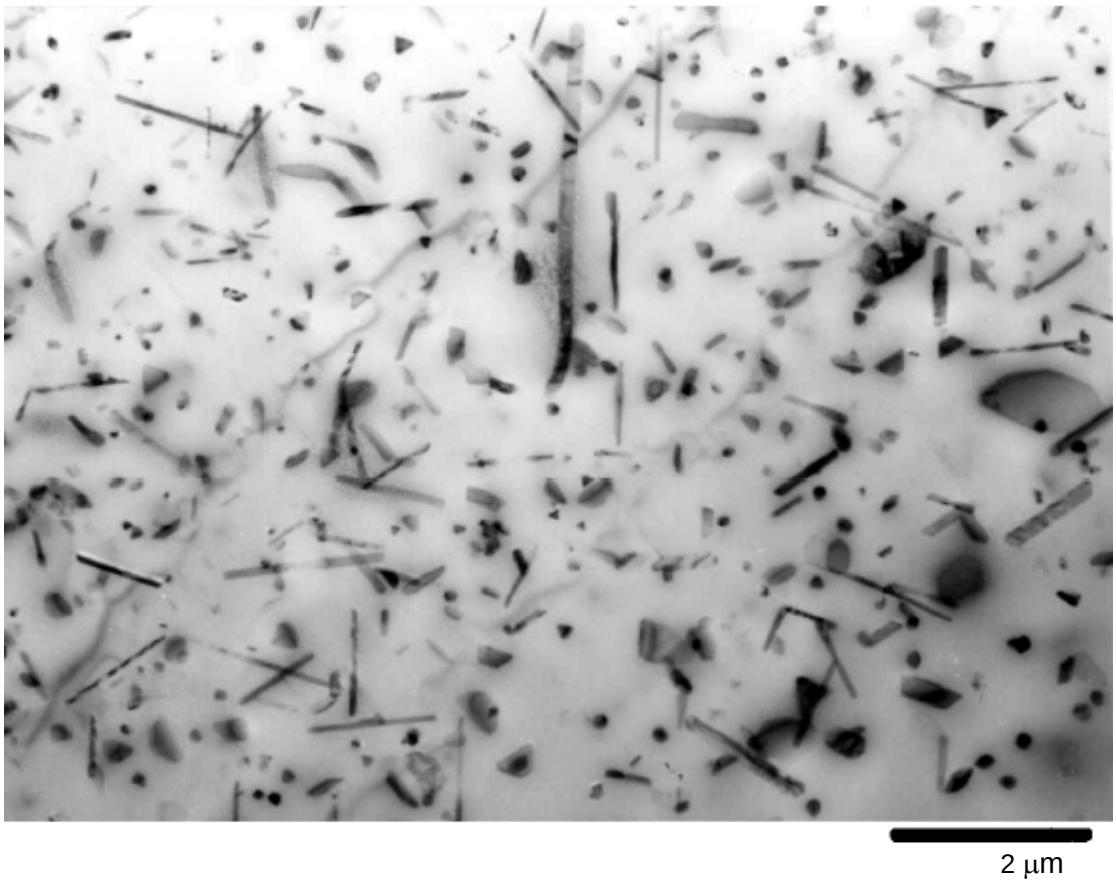

Fig. 1 TEM micrograph of the Al-Si alloy heated at 5 °C/min to the end of the precipitation effect (370°C) and subsequently aged for 5 min at 370°C. Note the various shapes of the Si precipitates.

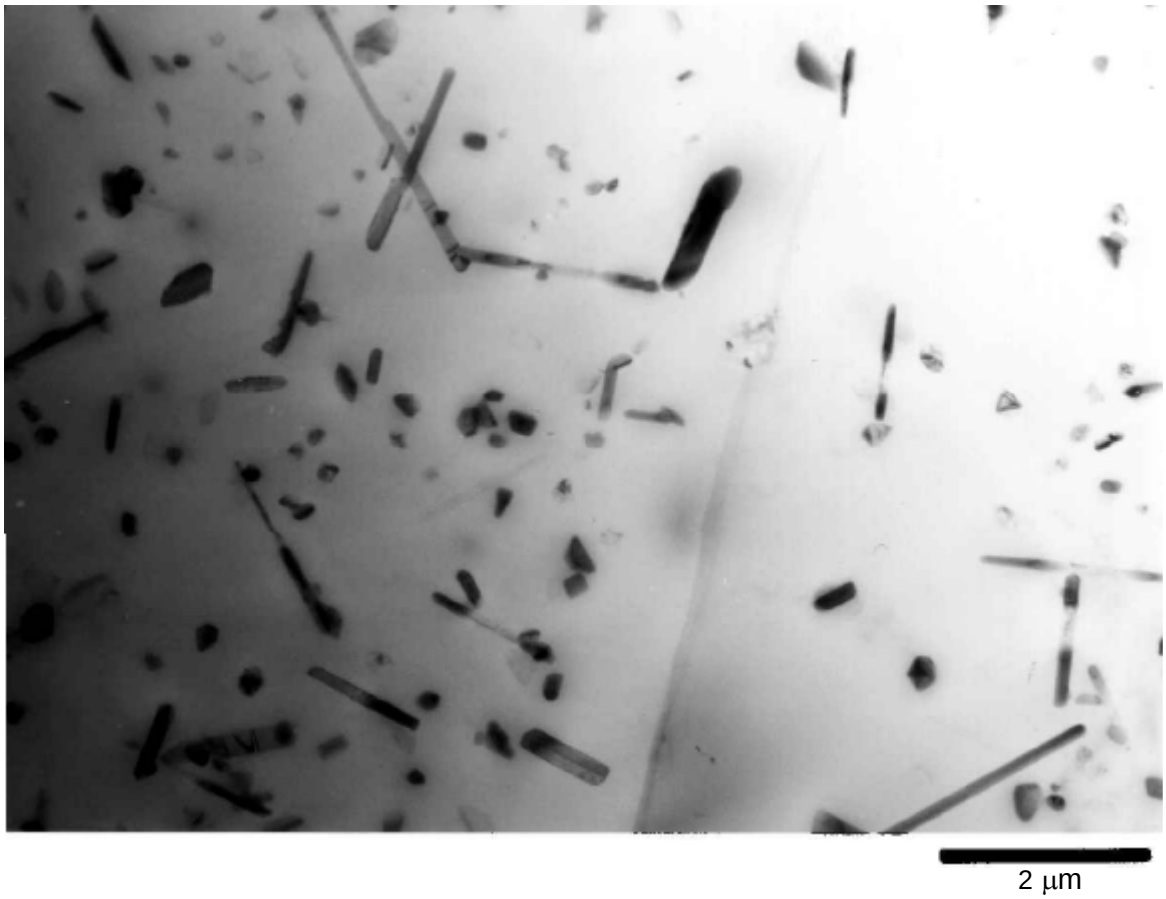

Fig. 2 TEM micrograph of the Al-Si alloy heated at 5 °C/min to the end of the precipitation effect (370°C) and subsequently aged for 24 h at 370°C. Note the grain boundary and a very limited precipitate free zone around it.

For further confirmation of this result we will compare the enthalpy of the samples aged for 5 min and for 24 h. As at the end of the exothermic DSC effect per definition neither net precipitation nor dissolution occurs, the Si concentration in the Al-rich phase should correspond to the (metastable) equilibrium concentration, and the ageing treatment at 370°C can only result in further precipitation if the metastable equilibrium concentration changes during the coarsening of the Si precipitates. Thus, the finite sizes of the precipitates influence the enthalpy of the samples in two ways: i) the interfacial energy reduces the effective average enthalpy of formation of a mole of Si precipitates, ΔH_{eff}, to ΔH_{sol} - $E_{Si/Al}$, and ii) the (metastable) solubility, c_{Si}' , will be increased, resulting in less Si precipitating. If the regular solution model is valid, c_{Si}' can be estimated from:

$$c'_{Si}(T,r) = c_\infty \exp\left(-\frac{\Delta H_{sol} - E_{Si/Al}(r)}{k_B T}\right) \qquad (13)$$

Thus the enthalpy of a sample with finite precipitates minus that of a sample with infinitely large precipitates is given by:

$$\Delta H(r) - \Delta H(r=\infty) = c'_{Si}(T,r)\left[\Delta H_{sol} - E_{Si/Al}(r)\right] - c_{Si}(T)\Delta H_{sol} \qquad (14)$$

It follows that the difference between the total heat effect of dissolution, ΔQ_d, of precipitates of radius r_1 compared to that of precipitates with radius r_2 is:

$$\Delta Q_d(r_2) - \Delta Q_d(r_1) = c'_{Si}(T, r_2)\left[\Delta H_{sol} - E_{Si/Al}(r_2)\right] - c'_{Si}(T, r_1)\left[\Delta H_{sol} - E_{Si/Al}(r_1)\right] \quad (15)$$

Evaluation of Eq. 13 and 15 shows that for the present samples aged for 5 min (2r = 117 nm) and for 24 h (2r = 164 nm) this difference amounts to 6 J/mol (again only equiaxed particles are considered).

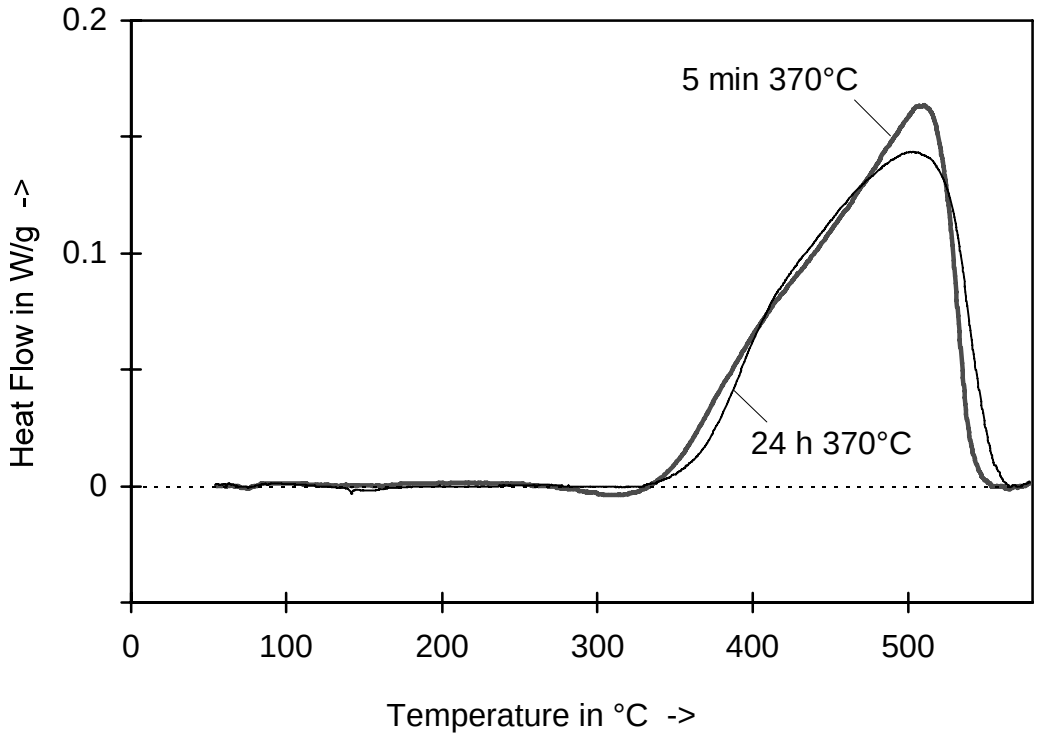

Fig. 3 DSC curves (β = 20°C/min) of Al-1at%Si samples which had been heated at 5°C/min to the end of the precipitation effect and subsequently aged for 5 min or for 24 h at 370°C.

The heat effects due to dissolution of the Si precipitates were measured by DSC experiments performed at a heating rate of 20 °C/min. As expected, these experiments show one single endothermic effect due to the dissolution of Si precipitates (see Fig. 3)[†]. ΔQ_d is marginally higher for the sample aged for 24 h: 491±4 J per mole alloy as compared to 485 J/mol for the sample aged for 5 min. Although this difference is quite small and hence difficult to measure, the different shapes of the dissolution curves in Fig. 3 clearly indicate that the sizes of the precipitates present in

[†] However, between 290 and 330°C a very small exothermic effect is observed for the sample which was aged for 5 min at 370°C (see Fig. 3). This effect is attributed to precipitation of some of the small amount of Si which remained in solution after ageing at 370°C. The magnitude of this effect is negligible when compared to the effects discussed here.

the two samples are significantly different. From the data on ΔQ_d three important conclusions can be drawn. Firstly, as the equilibrium solubility at 370°C is about 0.14at%Si, theoretically $\Delta Q_d \approx 0.0086 \times \Delta H_{sol}$ = 465±30 J/mol. This corresponds well with the experimental data, confirming that all Si has precipitated. Secondly, by using $E_{Si/Al}(r_1)/E_{Si/Al}(r_2) = r_2/r_1 = 164/117$ (from Eq. 12 and the TEM experiments) with Eqs. 13 and 15, the difference, 6±4 J per mole alloy, results in $E_{Si/Al} = 0.9 \pm 0.5$ kJ/mol. Thus, the determination of $E_{Si/Al}$ from the ΔQ_d data in combination with Eqs. 13 and 15 yields the same result as the one obtained from TEM data in combination with Eq. 12. Thirdly, a possible contribution of elastic energy due to misfit of Si particles in the Al-matrix to the enthalpy would influence the determination of $E_{Si/Al}$ from the ΔQ_d data, whilst it would not influence the determination from the TEM data. As both experiments yield the same results, it can be concluded that elastic energy is negligible.

According to Eq. 13, the determined value of $E_{Si/Al}$ causes a very small increase of the solubility. Thus it is justified to use the equilibrium solubility and neglect the Gibbs-Thomson effect.

4.2 Isothermal calorimetry

In Fig. 4 isothermal calorimetry experiments on furnace cooled samples at temperatures in the range 190-230°C are presented. The curves are normalised with respect to the maximum in the main exothermic heat effect which occurs between 220 and 12 ks for T between 180 and 260°C. The exothermic heat flow in these experiments and in the subsequent DSC experiments is interpreted to be due to precipitation of Si. In the same figure fits based on Eqs. 3, 4, 5 and 9 are presented. Following results of earlier experiments on Al-6Si (Starink and Zahra 1997a), two processes with n = ½ and n = 1½ are chosen for these fits. Fig. 5 shows schematically how the two processes contribute to the overall effect. The parameters k_o, E_{iso} and η_i for both processes and f (i.e. a total of 7 parameters) were adjusted to obtain the best fits. However, as has been noted before (Starink and Zahra 1997a), the choice of η_i for the first process (n = ½) has very little influence on the fitted curves. Hence, we have assumed that η_i for the two processes is equal, and the effective number of adjustable parameters decreases to 6. Following earlier work (Starink and Zahra 1997a), f was chosen as 0.17, except for the highest temperature for which f = 0.15 results in a significantly better fit. The parameters for the best fits in Fig. 4 are presented in Table 1. Comparison of fits and experimental data in Fig. 4 shows a very good correspondence.

4.3 DSC

In Fig. 6 DSC curves of the Al-6Si alloy at heating rates between 1.25 and 40 °C/min are presented along with fits based on Eqs. 3, 6, 9 and 10 in which again two processes with n = ½ and n = 1½ are used. Here, the parameters k_c, E_{eff} and η_i for both processes together with f were adjusted to obtain the best fits. Again η_i for the first process has very little influence on the overall result and the η_i values for the two processes are taken equal. Also E_{eff} is taken equal for the two processes. For most curves f could be taken equal to the value of f obtained in the isothermal experiments (0.17). However, this proved unsatisfactory for the highest heating rate (40°C/min), and for this fit f was reduced to 0.02. The parameters for the best fits in Fig. 6 are presented in Table 2. Also for this

figure comparison of fits and experimental data shows a very good correspondence. Fig. 7 shows schematically how the two processes contribute to the overall DSC effect.

Table 1 Parameters for best fit of isothermal calorimetry curves of furnace-cooled Al-6Si (Fig. 4).

	n	k_o (s^{-1})	E_{iso} (kJ/mol)	η_i
process 1	½	4938	89.7	1
process 2	1½	2040	79	1

Table 2 Parameters for best fit of DSC curves of Al-6Si (Fig. 6).

	s	k_c (s^{-1})	E_{eff} (kJ/mol)	η_i
process 1	½	246469	93.5	2.2
process 2	1½	129364	93.5	2.2

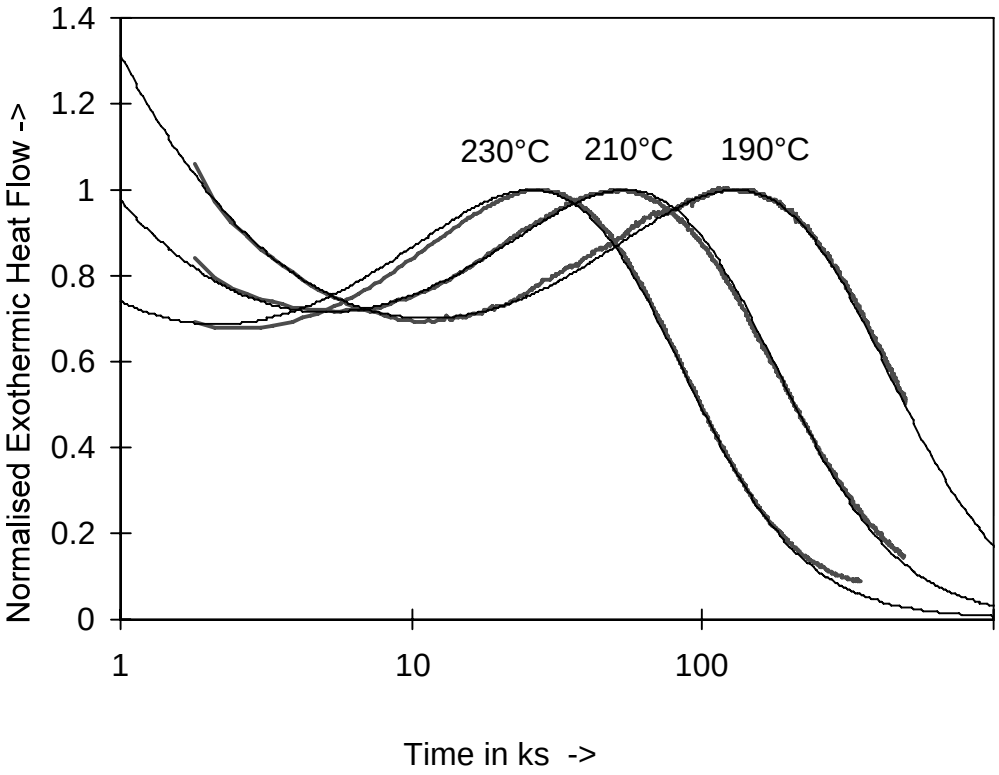

Fig. 4 Isothermal calorimetry curves of the furnace-cooled Al-6Si alloy at temperatures 190 to 230°C (thick grey lines) with fits obtained with parameters presented in Table 1.

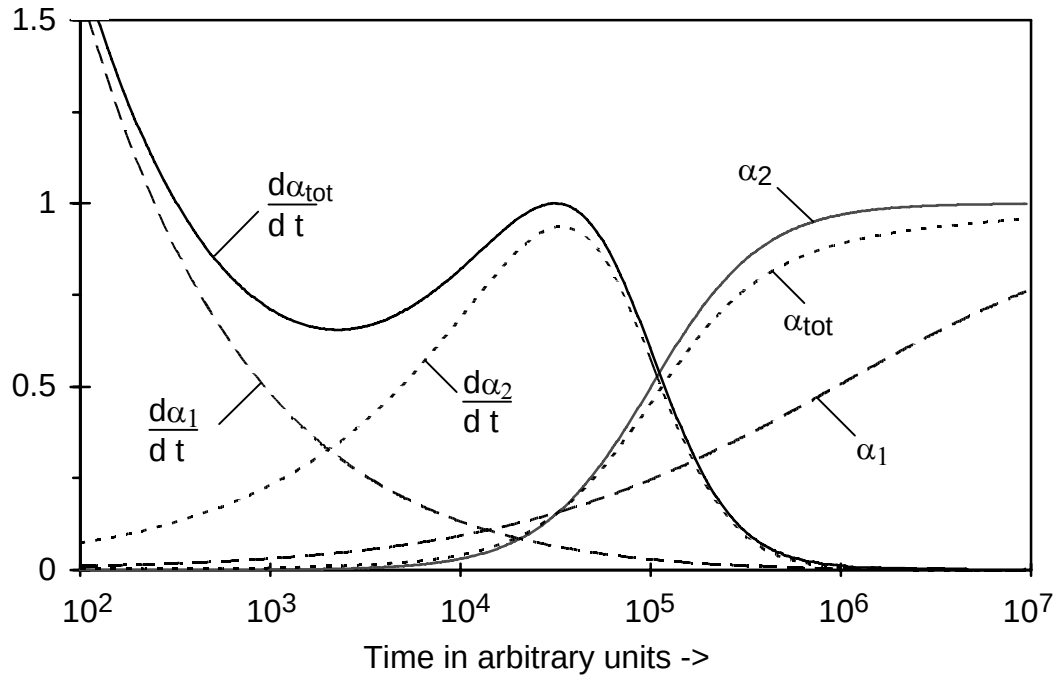

Fig. 5 Schematic representation of the contributions of the two processes to the calorimetry curve for Al-6Si.

4.4 Validity of the model

The comparisons of experimental results and fits presented in the previous section generally show a very good correspondence: all essential features of the curves can be reproduced by using the same basic model with two processes operating: i) precipitation via growth of large Si particles (n = s = ½) and ii) precipitation on small pre-existing nuclei (n = s = 1½). Generally f could be taken as constant but had to be adjusted separately for the highest heating rate (40°C/min) and for the highest isothermal temperature. The absence of a process with n = 2½ indicates that for all T-t paths studied, nucleation of precipitates during the reaction is negligible as compared to the amount of precipitates that exist at the start of the reaction. This is different from water-quenched Al-1at%Si and Al-6at%Si alloys for which best fits do include a process with n ≈ 2.5 (Starink and Zahra 1997a).

As the cooling procedures after solution treatment for the two types of experiments were somewhat different, it is not unexpected that the kinetic parameters like E_{iso} and E_{eff} differ slightly for the two T-t paths. The obtained activation energies compare well with activation energies for Si precipitation reported elsewhere[‡] (Van Rooyen and Mittemeijer 1989, Starink 1996). However, in

[‡] However, for furnace-cooled Al-6Si the activation energy of 79 kJ/mol obtained for process 2 is lower than the value obtained from an Arrhenius plot of the times at the peak of the exothermic heat flow for T ≤ 210, which we have reported as being 91 kJ/mol (Starink and Zahra 1997d). This difference is related to a curvature in the Arrhenius plot in combination with the different temperature intervals over which the analysis is performed (190-230°C in the present work, and 180-210°C in Starink and Zahra 1997d). This point is further discussed in Starink and Zahra 1997d.

terms of understanding of the kinetics, the values of the impingement exponent η_i obtained for the two T-t paths are more important. Firstly, it is noted that these values are totally incompatible with JMAK kinetics, as this type of kinetics predicts infinitely large values of η_i. Instead, the value $\eta_i = 1$ as obtained for the isothermal experiments conforms to the value predicted by the Austin-Rickett (AR) equation (see Austin and Rickett 1939, Lee and Kim 1990, Starink 1997), whilst the value obtained for the linear heating experiments, although different, is closer to the one predicted by the AR than to the one for JMAK kinetics. It has in fact been shown before (Starink 1997) that many precipitation reactions, including precipitation in quenched Al-Si alloys, conform quite well to the AR equation.

The above observations in general show that the model presented in Section 3 is sound and can describe both the isothermal and the non-isothermal kinetics of the process studied to a high degree of accuracy. Also for precipitation in Al-Mg and Al-Cu alloys the model provides good fits (Starink and Zahra 1997b, Starink and Zahra 1997c, Starink and Zahra 1997e). Thus the present model is well suited for analysis of isothermal and linear heating experiments in terms of the basic processes occurring. However, the difference between the η_i parameters for the two T-t paths has until now remained unexplained. This point is currently under investigation.

Conclusions

Isothermal calorimetry and DSC experiments have been performed on slowly cooled Al-6at%Si samples and the experiments have been compared to a novel theory of nucleation and growth type reactions. The theory incorporates nucleation, growth and impingement, takes account of temperature dependent solubility, and distinguishes between diffusion controlled growth and linear growth, but neglects coarsening. The results are summarised as follows.

- The theory with two processes operating yields very good fits to both types of experiments, following all main features of the experimental curves. The two processes concerned correspond to growth of large Si particles ($s = n = ½$) and growth of small nuclei ($s = n = 1½$).
- JMAK kinetics fails to fit the experiments.
- The later stages of the exothermic effect in the DSC experiments and even the dissolution part of the curve can be fitted well by the theory.
- The influence of the Gibbs-Thomson effect is estimated via particle size determinations (from TEM) and differences in the heats of dissolution of Si particles (measured by DSC). Both methods indicate that for the Al-Si alloy the Gibbs-Thomson effect has little influence on the solubility.

Acknowledgements

This work is financed in part by the EC Human Capital and Mobility project. Mr. C. Zahra is thanked for performing DSC experiments.

References

Austin, J.B., and Rickett, R.L., 1939, *Trans. Am. Inst. Min. Engrs.* 135, 396.

Christian, J.W., *The Theory of Transformation in Metals and Alloys*, 2nd ed., Part 1, 1975 (Oxford, UK: Pergamon Press).

Cumbrera, F.L., and Sanchez-Bajo, F., 1995, *Thermochim. Acta* 266, 315.

El Sayed, H., and Kovács, I., 1994, *Phys. Stat. Sol. A* 24, 123.

Erukhimovitch, V., and Baram, J., 1994, *Phys. Rev. B* 50, 5854.

Erukhimovitch, V., and Baram, J., 1995 *Phys. Rev. B* 51, 6221.

Ge Yu and Lai, J.K.L., 1996, *J. Appl. Phys.* 79, 3504.

Hornbogen, E., Mukhopadhyay, A.K., and Starke, E.A, 1992a, *Z. Metallkd.* 83, 577, 1992b *Scr. Metall. Mater.* 27, 733.

Krüger, P., 1993, *J. Phys. Chem. Solids* 54, 1549.

Lee, E.S., and Kim, Y.G., 1990, *Acta Metall. Mater.* 38, 1669.

Murray, J.L., and McAlister, A.J., 1984, *Bull. Alloy Phase Diagr.* 5, 74.

Ozawa, E., and Kimura, H., 1971, *Mater. Sci. Eng.* 8, 327.

Sakakibara, A., and Kanadani, T., 1990, *Mem. Faculty of Eng. Okayama University* 24, 11.

Saulnier, A., 1961, Mem. Sci. Rev. Met. 58, 615.

Sessa, V., Fanfoni, M., and Tomellini, M., 1996, *Phys. Rev. B* 54, 836.

Starink, M.J., 1996, *J. Mater. Sci. Lett.* 15, 1747.

Starink, M.J., 1997, *J. Mater. Sci.* 32, 4061

Starink, M.J., and Zahra, A.-M., 1996, *Aluminium Alloys: Their Physical and Mechanical Properties*, ICAA-5 Conference Proceedings, Grenoble, France, *Mater. Sci. Forum* 217-222, 795.

Starink, M.J., and Zahra, A.-M., 1997a, *Thermochim. Acta* 292, 159, 1997b, submitted to *Acta Mater*., 1997c, *J. Mater. Sci. Lett*., 16, 1613, 1997d, *Mater. Sci. Eng. A* 241, 277., 1997e, submitted to *J. Mater. Sci. Lett.*

Van Rooyen, M., and Mittemeijer, E.J., 1989, *Metall. Trans. A* 20, 1207.

Woldt, E., 1992, *J. Phys. Chem. Solids* 53, 521.

References

1 J.W. Christian, The Theory of Transformation in Metals and Alloys, 2nd ed., Part 1 (Pergamon Press, Oxford, UK, 1975).
2 F.L. Cumbrera and F. Sanchez-Bajo, *Thermochim. Acta* 266 (1995) 315.
3 V. Sessa, M. Fanfoni and M. Tomellini, *Phys. Rev. B* 54 (1996) 836.
4 Ge Yu and J.K.L. Lai, J. Appl. Phys. 79 (1996) 3504
5 Eon-Sik Lee and Young G. Kim, *Acta Metall. Mater.* 38 (1990) 1669.
6 M.J. Starink, *J. Mater. Sci.*, J. Mater. Sci., 1997, vol. 32, 4061; M.J. Starink, *J. Mater. Sci.*, 2001, 36, pp. 4433-4441
7 V. Erukhimovitch and J. Baram, *Phys. Rev. B* 50 (1994) 5854.
8 V. Erukhimovitch and J. Baram, *Phys. Rev. B* 51 (1995) 6221.
9 J.B. Austin and R.L. Rickett, *Trans. Am. Inst. Min. Engrs.* 135 (1939) 396.
10 M.J. Starink and A.-M. Zahra, *Thermochim. Acta.*, 1997, vol. 292, pp. 159-168
11 M.J. Starink and A.-M. Zahra, *J. Mater. Sci. Lett*., 1997, vol. 16, 1613-1615
12 M.J. Starink and A.-M. Zahra, *Acta Mater*., 1998, vol. 46, pp. 3381-3397
13 A. Sakakibara and T. Kanadani, *Mem. Faculty of Eng. Okayama University* 24 (1990) 11.
14 H. El Sayed and I. Kovács, *Phys. Stat. Sol. A* 24 (1994) 123.
15 E. Ozawa and H. Kimura, *Mater. Sci. Eng.* 8 (1971) 327.
16 M.J. Starink, *J. Mater. Sci. Lett.* 15 (1996) 1747
17 J.L. Murray and A.J. McAlister, *Bull. Alloy Phase Diagr.* 5 (1984) 74.
18 M.J. Starink and A.-M. Zahra, Proc. of ICAA-5, Grenoble, France, *Mater. Sci. Forum* 217-222, 1996, 795.
19 E. Woldt, *J. Phys. Chem. Solids* 53 (1992) 521.
20 P. Krüger, *J. Phys. Chem. Solids* 54 (1993) 1549.
21 M. van Rooyen and E.J. Mittemeijer, *Metall. Trans. A* 20 (1989) 1207.
22 A. Saulnier, Mem. Sci. Rev. Met. 58 (1961) 615
23 E. Hornbogen, A.K. Mukhopadhyay and E.A. Starke, Z. Metallkd. 83 (1992) 577
24 E. Hornbogen, A.K. Mukhopadhyay and E.A. Starke, *Scr. Metall. Mater*. 27 (1992) 733
25 A.-M. Zahra and M.J. Starink, *J. Mater. Sci*., 1999, vol. 34, pp. 1117-1127